

## **Additional File 1: Supporting information.**

### **Tripartite interactions of PKA catalytic subunit and C-terminal domains of cardiac Ca<sup>2+</sup> channel may modulate its $\beta$ -adrenergic regulation**

Shimrit Oz<sup>1,2,†</sup>, Tal Keren-Raifman<sup>1</sup>, Tom Sharon<sup>1</sup>, Suraj Subramaniam<sup>3</sup>, Tamara Pallien<sup>4</sup>, Moshe Katz<sup>1</sup>, Vladimir Tsemakhovich<sup>1</sup>, Anastasiia Sholokh<sup>4</sup>, Baraa Watad<sup>1</sup>, Debi Ranjan Tripathy<sup>1,3,†</sup>, Giorgia Sasson<sup>3</sup>, Orna Chomsky-Hecht<sup>3</sup>, Leonid Vysochek<sup>5</sup>, Maike Schulz<sup>4</sup>, Claudia Fecher-Trost<sup>6</sup>, Kerstin Zühlke<sup>4</sup>, Daniela Bertinetti<sup>7</sup>, Friedrich W. Herberg<sup>7</sup>, Veit Flockerzi<sup>6</sup>, Joel A. Hirsch<sup>3</sup>, Enno Klussmann<sup>4,8</sup>, Sharon Weiss<sup>1</sup>, Nathan Dascal<sup>1</sup>

<sup>1</sup>School of Medicine, Faculty of Medical and Health Sciences Tel Aviv University, Tel Aviv 6997601 Israel;

<sup>2</sup> Department of Neuroscience, The Ruth and Bruce Rappaport Faculty of Medicine, Technion – Israel Institute of Technology, Haifa 3109601, Israel;

<sup>3</sup> School of Neurobiology, Biochemistry and Biophysics, Faculty of Life Sciences, Tel Aviv University, Tel Aviv 6997601, Israel;

<sup>4</sup> Max-Delbrück-Center for Molecular Medicine in the Helmholtz Association (MDC), Berlin, Germany;

<sup>5</sup>Heart Center, Sheba Medical Center, Ramat Gan, 5262000 Israel;

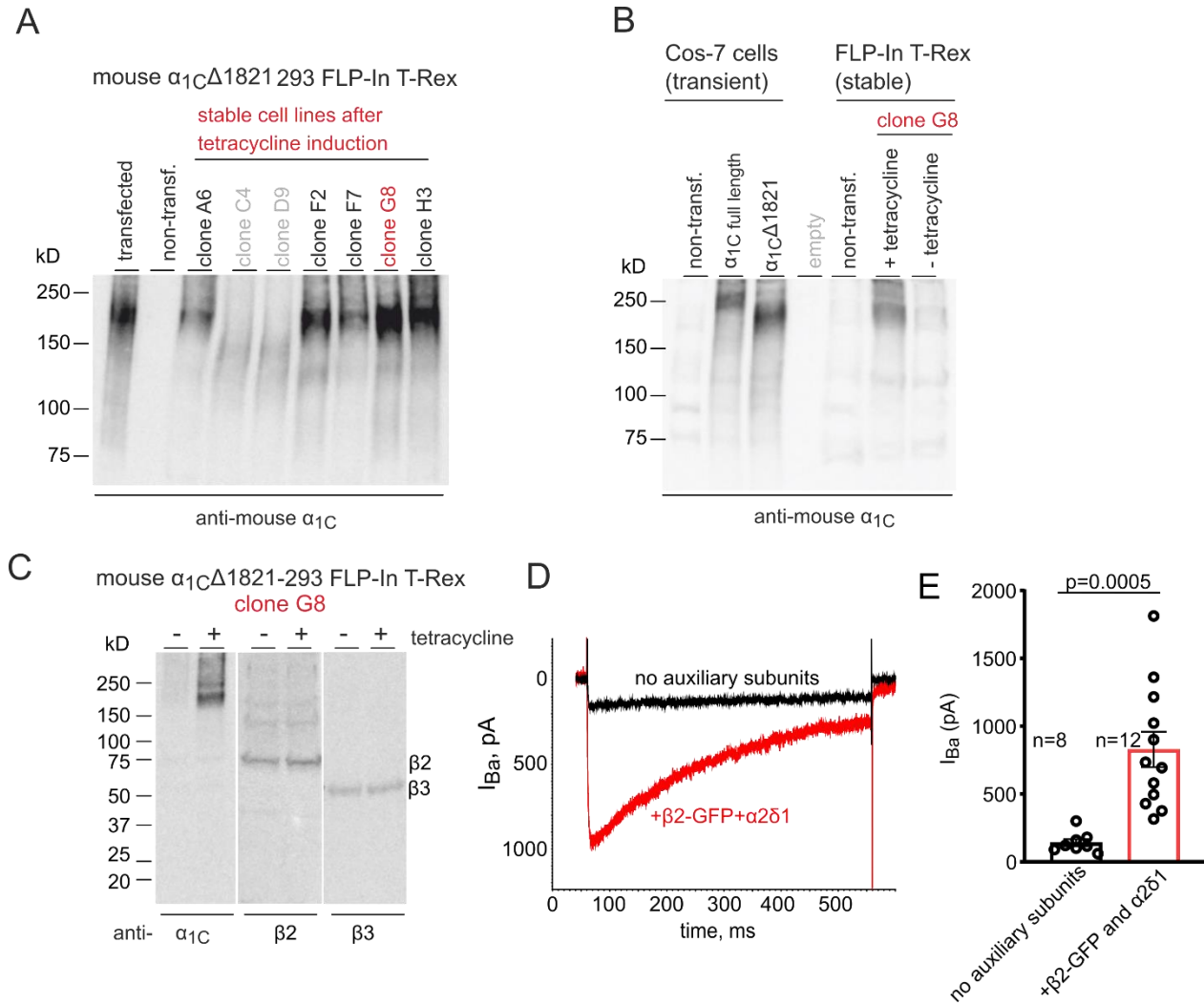
<sup>6</sup>Experimentelle und Klinische Pharmakologie & Toxikologie, Universität des Saarlandes, 66421 Homburg, Germany

<sup>7</sup>Department of Biochemistry, University of Kassel, Heinrich-Plett-Str. 40, 34132 Kassel, Germany

<sup>8</sup> DZHK (German Centre for Cardiovascular Research), partner site Berlin, Germany

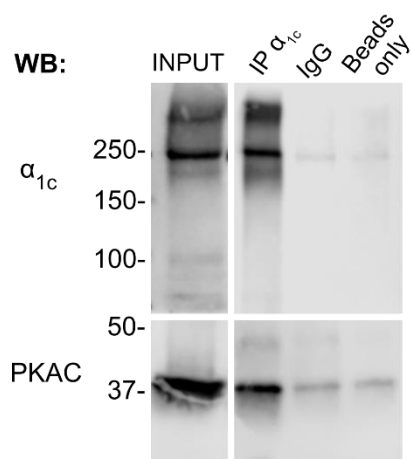
<sup>†</sup> Present address: National Forensic Science University, Radhanagar, Agartala, Tripura 799001, India

**Fig S1.**



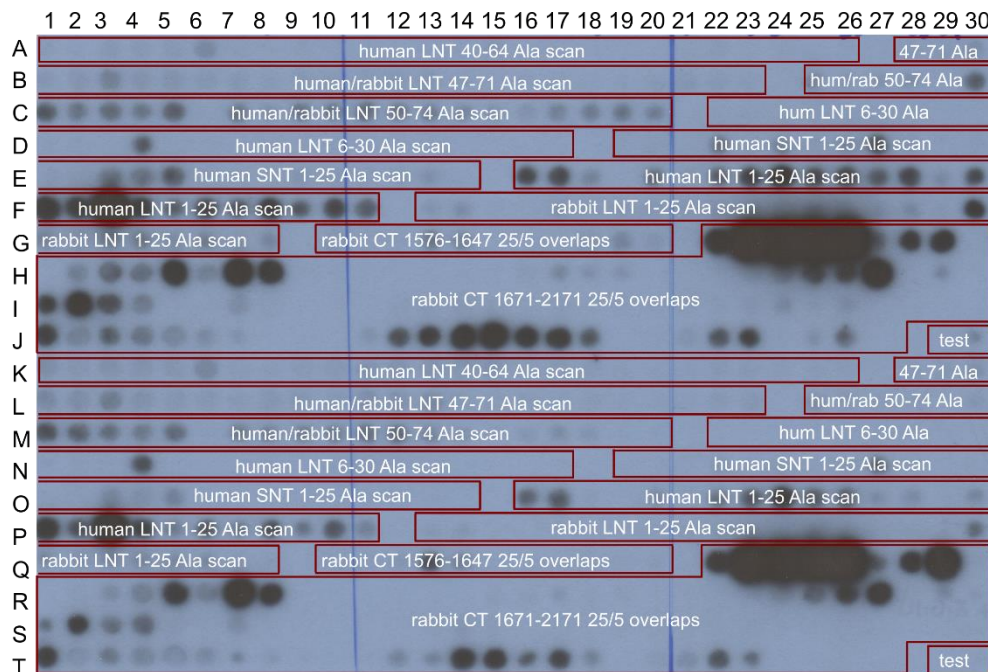
**Figure S1, related to Fig. 2. Generation of HEK293 cells stably transfected with  $\alpha_1$  truncated at 1821 and  $Ba$  currents in these cells.** *A*, Seven independent stable cell lines were generated, and tetracycline-induced Cav1.2 $\alpha_{1\Delta 1821}$  was detected by Western blot. Clone G8 had the highest  $\alpha_{1\Delta 1821}$  expression and was selected for all following experiments. *B* and *C*, Western blot analysis of full length  $\alpha_1$  vs.  $\alpha_{1\Delta 1821}$  in Cos-7 cells transiently expressing  $\alpha_1$  (*B*) and in the G8 cell line stably expressing  $\alpha_{1\Delta 1821}$  when induced by tetracycline (*C*). Note that these cells contain endogenous Cav $\beta_2$  and Cav $\beta_3$ , which probably contribute to the formation of the functional channel. *D*, Exemplary traces from tetracycline-induced G8 clone of typical  $Ba^{2+}$  current waveform, from a cell that did not express auxiliary subunits (black) and a cell transfected with DNAs of  $\alpha_{2\delta 1}$  and  $\beta_2$ -GFP (red). Currents were elicited by a voltage step from resting potential of -120 mV to 10 mV. Leak current subtraction was performed on-line using a P3 protocol (3 sub-pulses of opposite polarity). *E* Summary of  $Ba^{2+}$  current amplitudes measured as in (*D*) in tetracycline-induced G8 clone cells without (black) and with (red) cotransfection of the auxiliary subunits. Mean $\pm$ SEM are shown, with number of cells above the bars. Statistics: unpaired t-test.

**Fig. S2**



**Figure S2, related to Fig. 2. PKAC co-immunoprecipitates with  $\alpha_1$  from rat heart.** Summary of a representative experiment (out of three). Endogenous  $\text{Ca}_v1.2\text{-}\alpha_1$  (denoted here as  $\alpha_{1c}$ ) was immunoprecipitated from the lysates of rat's left ventricles, and PKAC co-immunoprecipitation was detected. Immunoprecipitation with unrelated rabbit IgG and no antibody (beads only lane) were used as negative controls. The original gels are available in Additional File 2/Original gels for Fig. S2.png

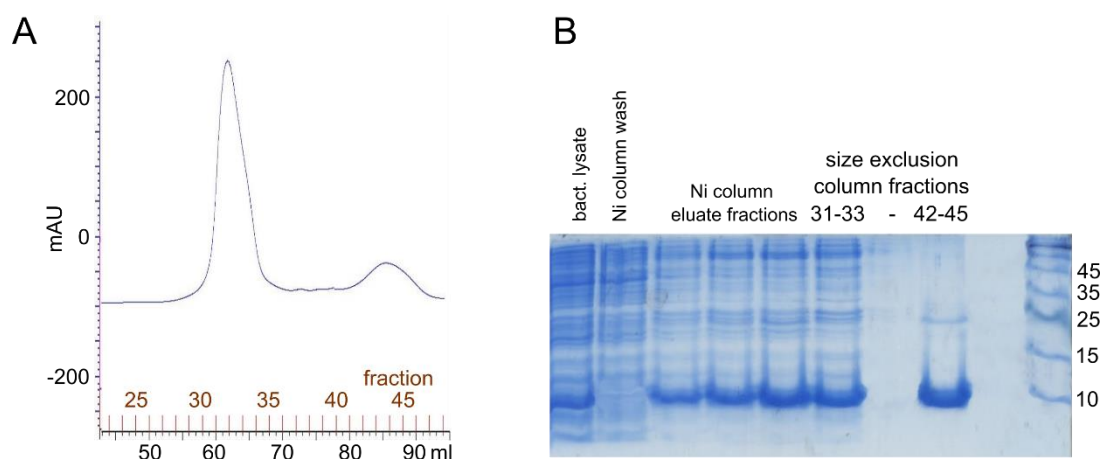
**Fig S3.**



**Figure S3, related to Fig. 3. The full peptide array membrane of  $\alpha_1$  N- and C-terminal 25 a.a. peptides.**

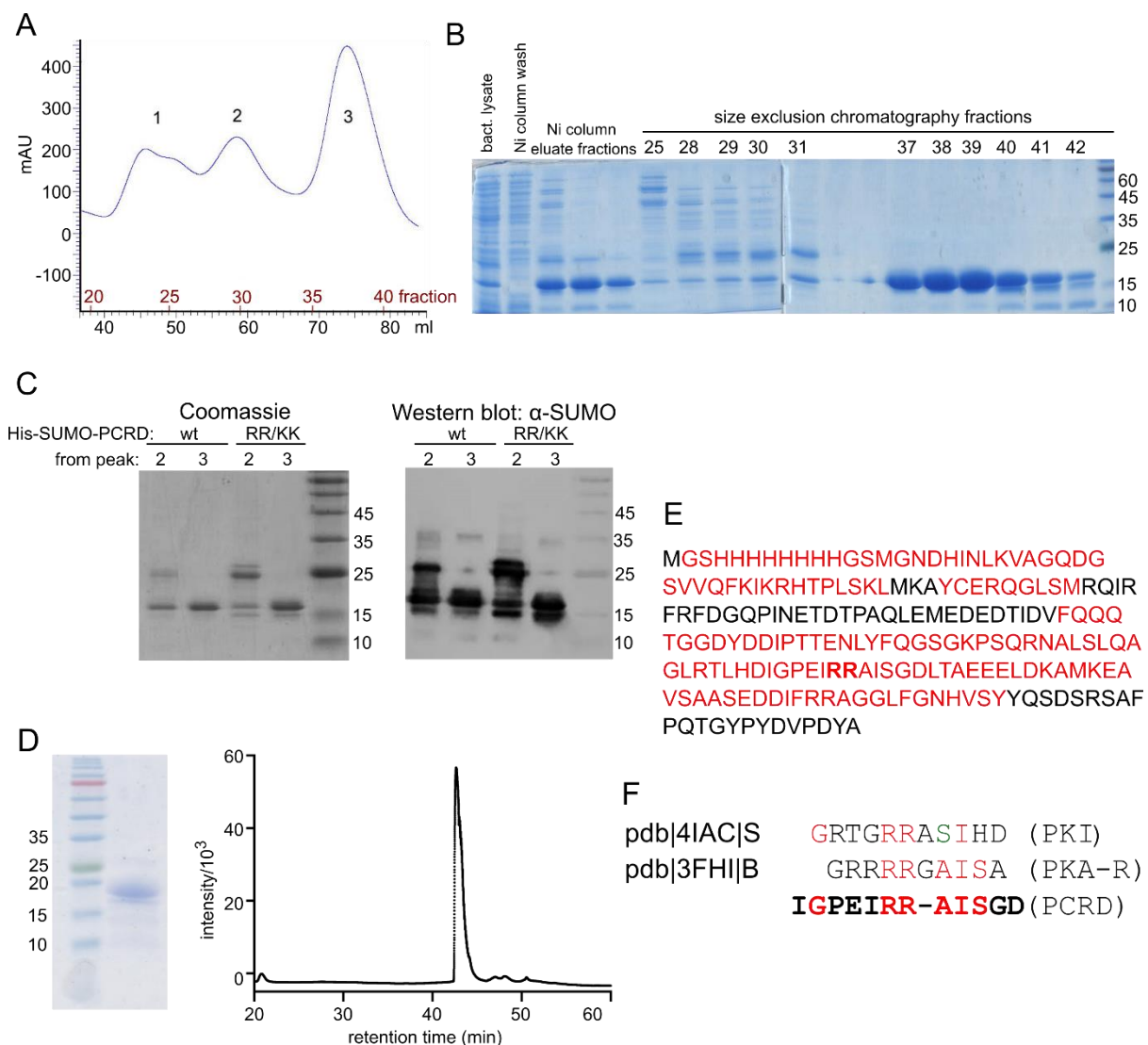
Lines K-T present a duplicate of the array of lines A-J. The image shows the result of the overlay with 0.1  $\mu$ M PKAC (lines A to J) or 0.02  $\mu$ M PKAC (lines K-T), followed by PKA detection with PKAC antibody (1:1000) and secondary anti-rabbit antibody (1:40000). Each of the 25 spot-long framed stretches in A1-G8 shows alanine scans of the indicated NT peptides. LNT, long-NT isoform; SNT, short-NT isoform. The notation human/rabbit corresponds to stretches of 100% homology between human and rabbit  $\alpha_1$ . In each stretch, the leftmost spot is the WT peptide and the following spots corresponds to alanine mutations of consequent a.a. (e.g. spot A2 is Ala mutant of the first a.a., spot A3 of the second a.a., and so on). Note that, although several strongly labeled spots are observed within the stretch corresponding to the human a.a. 1-25 peptide, the strongest spots correspond to some of the Ala mutations, and the WT peptide (E16) shows only a modest labeling. Moreover, the overlapping peptide a.a. 6-30, and the highly homologous rabbit 1-25 peptide, show no labeling. The part of the array after alanine scans, G10-J27, comprises 25-mer peptides with 20 a.a. overlaps (5 a.a. shift between peptides) corresponding to WT rabbit  $\alpha_1$  CT sequences. The major part of the CT, a.a. 1576-2171 (excluding the IQ domain, a.a. 1648-1670), is the same as shown in Fig. 2A. Note no labeling in the proximal CT, a.a. 1576-1647. The “test” peptides in spots J29 and J30 are unrelated to  $\alpha_1$ , ARNDQEGHILKMFPSTYVARNDQEG and WRNDQEGHILKMFPSTYVARNDQEG.

**Fig S4**



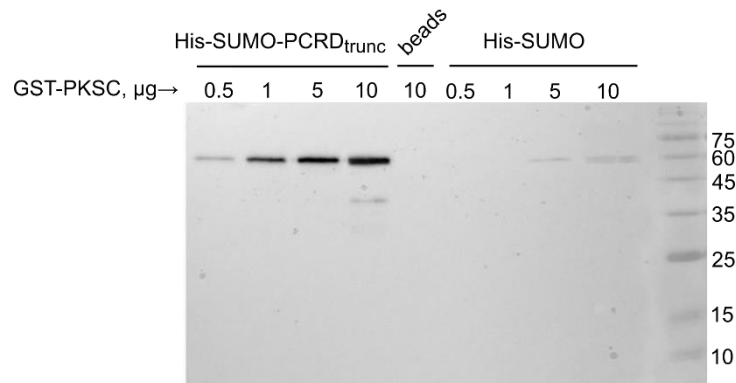
**Figure S4, related to Fig. 4. His-DCRD-Myc: purification from *E. coli*.** A, elution profile from the size exclusion chromatography column (16/60 Superdex 75). B, analysis of the proteins obtained at the different stages of His-SUMO-PCRD preparation and purification. Coomassie stain of SDS-PAGE (12% gel). Representative of at least 3 similar purifications.

**Fig S5**



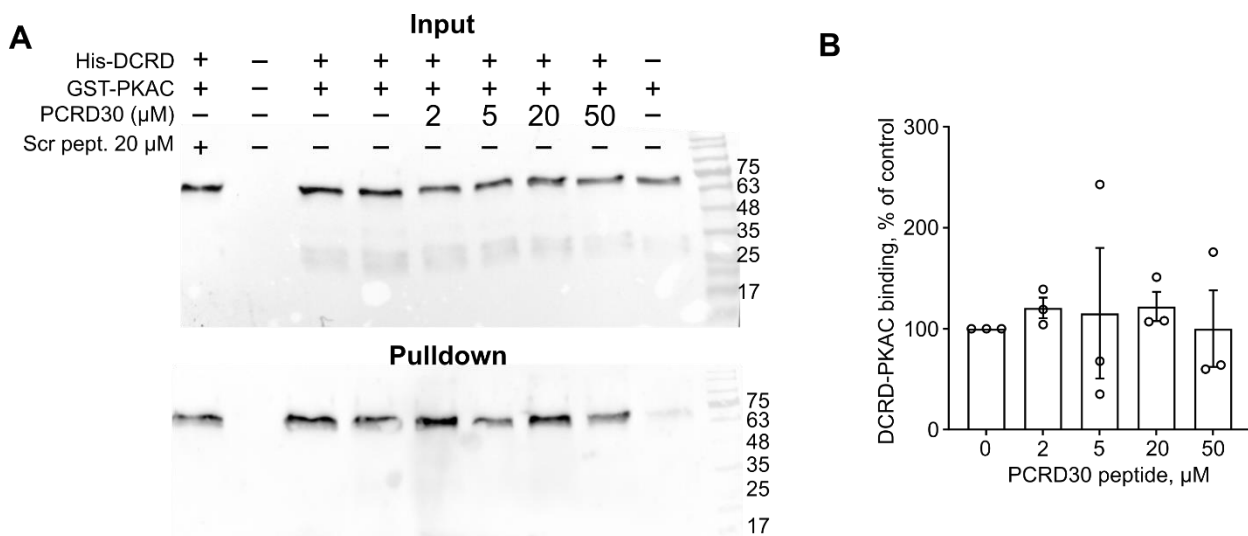
**Figure S5, related to Fig. 4. His-SUMO-PCRD: purification and analysis.** A, B, purification of His-SUMO-PCRD from *E. coli*. A, elution profile from the size exclusion chromatography column (16/60 Superdex 75). Representative of at least 3 similar purifications. B, analysis of the proteins obtained at the different stages of His-SUMO-PCRD preparation and purification. Coomassie stain of SDS-PAGE (12% gel). C, Western blot with anti-SUMO antibody of purified WT and RR/KK His-Sumo-PCRD proteins (two separate preparations, the elution profiles from the Superdex column were similar to that in A). The SUMO antibody recognizes both the long and the truncated forms of His-SUMO-PCRD, indicating that the N-terminal part of the protein is not proteolysed. D-E, fraction 28 of His-SUMO-PCRD<sub>trunc</sub> from a separate purification was analyzed by 12% SDS-PAGE and reverse phase HPLC (D), and trypsin/pepsin digestion followed by nano-LC MS/MS (E). The a.a. labeled in red color were present in the digestion products detected by the MS. F, alignment of PKAC-binding pseudosubstrate peptides from mouse/human PKI and mouse/bovine PKAR with the analogous segment of PCRD. Color coding (relative to PCRD): red, identical; green, similar. The full MS data are available via ProteomeXchange with identifier PXD057841.

**Fig S6**



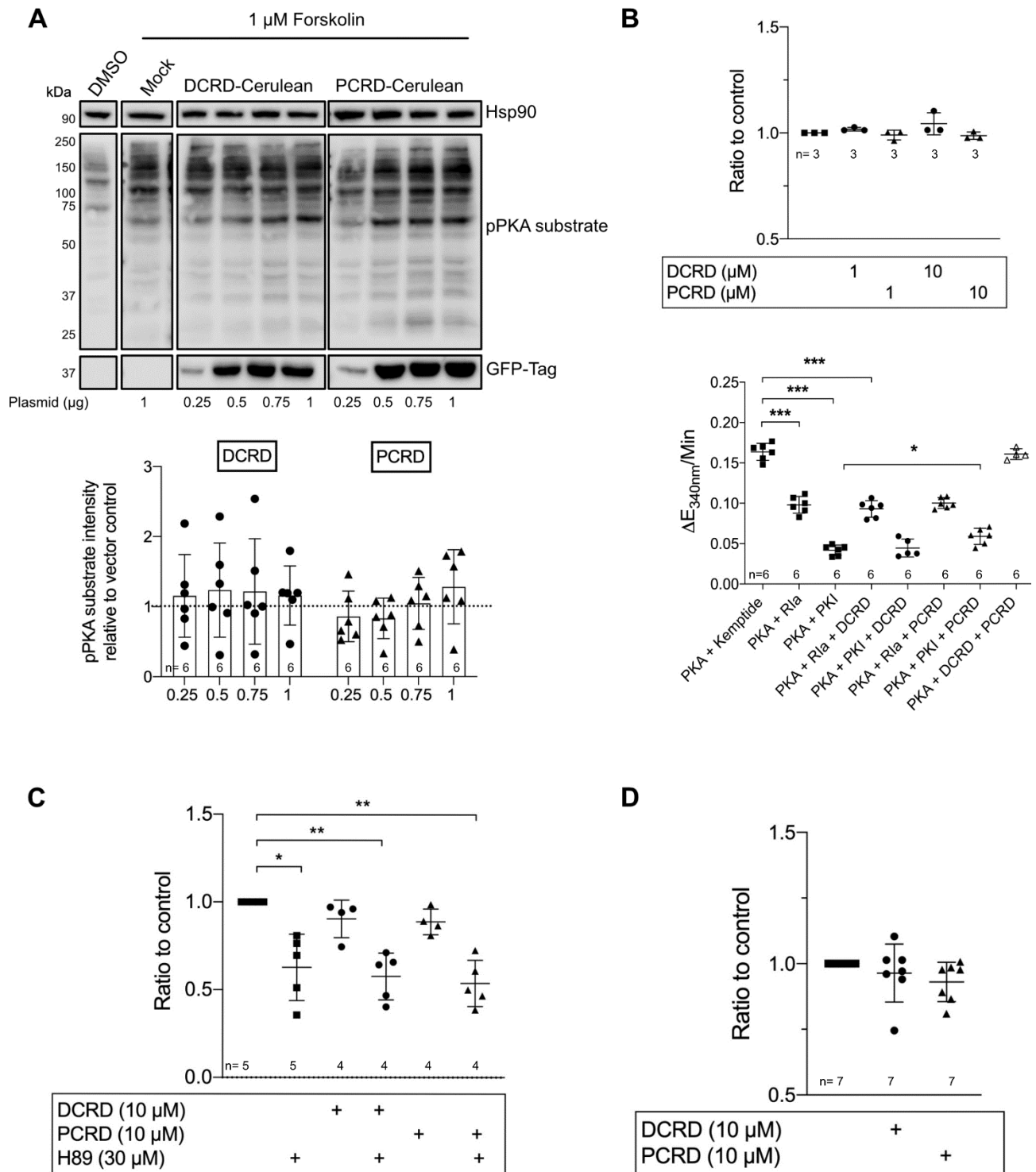
**Figure S6, related to Fig. 5. SUMO does not bind PKAC.** 1 µg of purified His-SUMO-PCRD<sub>trunc</sub> or His-SUMO were used to pull down the indicated amounts of GST-PKAC on Ni-NTA beads. The reaction volume was 300 µl. The image shows Western blot of the eluted proteins, detected with the PKA antibody. Representative of 2 experiments.

**Fig S7**



**Figure S7, related to Fig. 7. The PCR30 peptide does not reduce the interaction between His-DCRD and GST-PKAC.** **A**, results of a representative experiment, out of three. His-DRCD (2 µM) was pulled down on Ni-NTA beads in the presence or absence of GST-PKAC (250 nM) and absence or presence of PCR30 peptide (2-50 µM). Neither PCR30 nor scrambled (Scr) peptide altered the amount of GST-PKAC pulled down by His-DCRD. Control (no peptides present) was repeated as duplicate in each experiment. GST-PKAC was detected by GST antibody (1:500). **B**, summary of three experiments. DCRD-PKAC binding is presented as % of control (no PCR30 peptide). Results are presented as mean±SEM. The differences between the groups were not significant (Kruskal-Wallis multiple comparisons test, p=0.58).

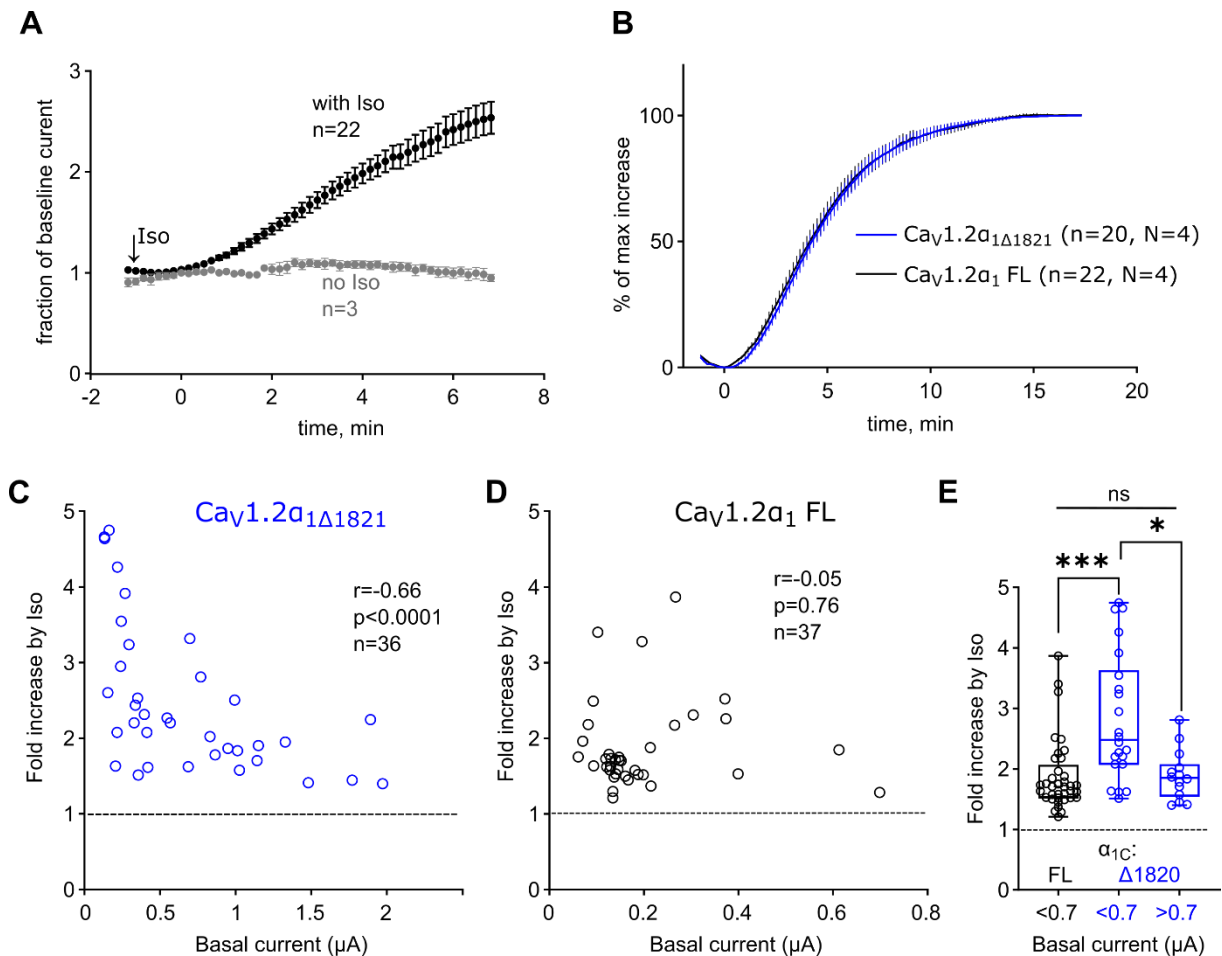
**Fig. S8**



**Figure S8. PCRD and DCRD do not alter the catalytic activity of PKAC.** A, the indicated amounts of DCRD- and PCRD-Cerulean plasmids were expressed in HEK293 cells and the amount of phosphorylated PKA substrate proteins was detected using anti-pPKA substrate antibody. The empty vector control (Mock) shows that the forskolin stimulation worked and induced phosphorylation of PKA substrates. The graph shows the mean ratio of the pPKA substrate signal  $\pm$  SD to the Mock control sample (n=6). B, in the Cook assay, 40 nM of human PKAC was incubated with the indicated concentrations of His-DCRD-Myc or His-SUMO-PCRD with 260  $\mu$ M Kemptide. The upper graph shows the ratio to the PKAC and Kemptide for only control measurements  $\pm$  SD



(n=3). For the lower graph, 30 nM PKA-R1 $\alpha$  or 30 nM PKI were added in the presence and absence of the channel fragments (10  $\mu$ M) (n = 6 independent measurements, n = 4 for DCRD/PCRD combination). C, ADP Glo Assay. 10  $\mu$ M of His-DCRD-Myc, His-SUMO-PCRD or 30  $\mu$ M H89 were incubated with 20 nM bovine PKAC and the resulting amount of ADP measured as luminescence signal. The graph shows the ratio to the control sample (PKAC + Kemptide)  $\pm$  SD (n=4). D, cumulative graph of the Cook Assay (B) and ADP Glo Assay (C). For statistics, Kruskal-Wallis test with Dunn's correction was applied. \*p  $\leq$  0.05, \*\* p  $\leq$  0.01, \*\*\* p  $\leq$  0.001.

**Fig. S9**

**Figure S9, related to Fig. 8.  $\beta 1\text{AR}$  regulation of full-length and truncated  $\text{Ca}_v1.2$ : kinetics of Iso effect and additional analysis of published results.** **A**, comparison of time courses of changes in  $I_{\text{Ba}}$  in cells expressing  $\text{Ca}_v1.2$  (full-length  $\alpha_1$ ,  $\beta_{2b}$  and  $\alpha_{2\delta}$ ),  $\beta 1\text{AR}$  and Rad, without Iso or with the addition of 200 nM Iso. In all cases, the cells were perfused with bath solution at a constant rate during the recording. Iso was added by perfusing from a separate tube that contained the drug (dissolved in the same solution), without changing the rate of flow. In all cells, the baseline  $I_{\text{Ba}}$  was allowed a 4–15 min period to stabilize, as illustrated in Fig. 8A. Zero-time point was chosen 1.17 min after the addition of Iso, to account for the perfusion system dead time and part of the physiological delay. In control cells not exposed to Iso, the zero-time point was chosen similarly, at least 1.17 min after baseline  $I_{\text{Ba}}$  stabilization. Data are presented as mean $\pm$ SEM. Note that in some cells that were exposed to Iso, the maximal increase was attained slower than in the others; therefore, in order to maintain the statistical relevance, only the initial 7 min after Iso are summarized. A complete kinetic analysis is shown in B. **B**, comparative analysis of the kinetics of Iso effects in  $\text{Ca}_v1.2\alpha_1 \text{ FL}$  and  $\text{Ca}_v1.2\alpha_{1\Delta 1821}$ . In each cell, the Iso-induced current increase at each time point was expressed as percent of the maximal increase in the same cell. In some cells the maximal effect was attained, and the recording was stopped, earlier than in others. To enable comparison at longer times, in such cells the missing data points at later times were assigned the value of 100%. Data are presented as mean $\pm$ SEM. There was no statistical difference between the two curves ( $p=0.112$  by two-way ANOVA). **C–E**, the relationship between baseline  $I_{\text{Ba}}$  and fold

increase by Iso – reanalyzing published data. The original data from Katz et al. paper [56] were analyzed in the same way as shown in Fig. 8, to seek for correlation between  $I_{Ba}$  and the extent of current increase caused by Iso (50  $\mu$ M Iso were used in this work). Oocytes expressed all  $Ca_v1.2$  subunits ( $\alpha_1$ ,  $\beta 2b$ ,  $\alpha 2\delta$ ),  $\gamma$  and  $\beta 1AR$ . *A* and *B*, correlation between basal  $I_{Ba}$  and fold increase by Iso in individual cells. Parameters of Spearman correlation analysis for the two distributions are shown in insets. Note that the amplitudes of  $I_{Ba}$  in  $Ca_v1.2$  with FL- $\alpha_1$  were smaller ( $<0.7 \mu A$ ) than for  $\alpha_{1\Delta 1821}$  (0.1-2  $\mu A$ ). *C*, Comparison of the differences in Iso-induced increase in  $I_{Ba}$  of  $\alpha_{1\Delta 1821}$  and  $\alpha_1$ -FL for basal  $I_{Ba}$  of small-intermediate and high amplitudes. In this series of experiments large ( $>0.7 \mu A$ ) currents were observed only with  $\alpha_{1\Delta 1821}$ . Despite the smaller number of measurements, the tendency observed in experiments of Fig. 8E is also observed here: the Iso-induced increase in  $I_{Ba}$  is larger for  $\alpha_{1\Delta 1821}$  than in  $\alpha_1$ -FL for smaller currents, but not for larger  $\alpha_{1\Delta 1821}$  currents.

**Table S1: Antibodies used**

Antibody	Mono or polyclonal, organism	Source and cat. #	Validation
Ca <sub>v</sub> 1.2 ( $\alpha_1$ )	Rabbit; poly	ACC003, Alomone	See published papers [9, 29], and references in: <a href="https://www.alomone.com/p/anti-cav1-2-antibody/ACC-003">https://www.alomone.com/p/anti-cav1-2-antibody/ACC-003</a>
PKA $\alpha$ cat Antibody (C-20) (PKA $\alpha$ )	Rabbit; poly	Santa Cruz sc-903	See references in: <a href="https://www.scbt.com/p/pkaalpha-cat-antibody-c-20# Citations">https://www.scbt.com/p/pkaalpha-cat-antibody-c-20# Citations</a>
SCN1A (Na <sub>v</sub> 1.1)	Rabbit; poly	Alomone ASC-001	See Fig. 2 and references in: <a href="https://www.alomone.com/p/anti-nav1-1-2/ASC-001?gad_source=1&amp;gclid=Cj0KCQiA4Y-sBhC6ARIsAGXF1g4wzGVTJo2MeLTts55N-guKzkUDe8upmrAyF2ZVPCnEJTE-zLqIU1saAhdXEALw_wcB">https://www.alomone.com/p/anti-nav1-1-2/ASC-001?gad_source=1&amp;gclid=Cj0KCQiA4Y-sBhC6ARIsAGXF1g4wzGVTJo2MeLTts55N-guKzkUDe8upmrAyF2ZVPCnEJTE-zLqIU1saAhdXEALw_wcB</a>
HA-Tag Antibody (F-7)	Mouse; mono	Santa Cruz Sc-7392	See references in: <a href="https://www.scbt.com/p/ha-probe-antibody-f-7">https://www.scbt.com/p/ha-probe-antibody-f-7</a>
Anti-His <sub>6</sub> -Peroxidase	Mouse; mono	11965085001 Roche	See references in: <a href="https://www.sigmaaldrich.com/IL/en/product/roche/11965085001">https://www.sigmaaldrich.com/IL/en/product/roche/11965085001</a>
GFP	poly; rabbit	G1544 Sigma Aldrich	See references in: <a href="https://www.sigmaaldrich.com/specification-sheets/112/516/G1544-BULK_SIGMA_.pdf">https://www.sigmaaldrich.com/specification-sheets/112/516/G1544-BULK_SIGMA_.pdf</a>
Cav $\beta$ 2	Rabbit; poly	Generated in-house	See papers: [78-81]
Cav $\beta$ 3	Rabbit; poly	Generated in-house	
Peroxidase AffiniPure™ Goat Anti-Rabbit IgG (H+L)	Goat; poly	Jackson 111-035-144	See references in: <a href="https://www.jacksonimmuno.com/catalog/products/111-035-144/Goat-Rabbit-IgG-HL-Horseradish-Peroxidase">https://www.jacksonimmuno.com/catalog/products/111-035-144/Goat-Rabbit-IgG-HL-Horseradish-Peroxidase</a>
Peroxidase IgG Fraction Monoclonal Mouse Anti-Rabbit IgG, light chain specific	Mouse; mono	Jackson 211-032-171	See references in: <a href="https://www.jacksonimmuno.com/catalog/products/211-032-171">https://www.jacksonimmuno.com/catalog/products/211-032-171</a>
6x-His Tag Monoclonal Antibody	Mouse; mono	Invitrogen MA1-135	See references in: <a href="https://www.thermofisher.com/antibody/product/6x-His-Tag-Antibody-clone-4E3D10H2-E3-Monoclonal/MA1-135">https://www.thermofisher.com/antibody/product/6x-His-Tag-Antibody-clone-4E3D10H2-E3-Monoclonal/MA1-135</a>
Myc-Tag (9B11) Mouse mAb	Mouse; mono	Cell signaling technologies 2276	See references in: <a href="https://www.cellsignal.com/products/primary-antibodies/myc-tag-9b11-mouse-mab/2276">https://www.cellsignal.com/products/primary-antibodies/myc-tag-9b11-mouse-mab/2276</a>